The University of Michigan • Office of Research Administration
Ann Arbor, Michigan

06343-5-P

July 9, 1965

GPO PRICE $ _____

CFSTI PRICE(S) $ _____

Office of Grants and Research Contracts
Code SC
Office of Space Sciences and Applications
National Aeronautics and Space Administration
Washington, D. C.   20546

Hard copy (HC) ___ 2.00 ___

Microfiche (MF) ___ .50 ___

Subject: Letter Progress Report of Work under Contract No. NASr-54(06) for
           the Period 1 March 1965 to 31 May 1965

Gentlemen:

This status report covers work during the period from 1 March 1965
to 31 May 1965 under Contract NASr-54(06), Man-Machine Performance Measure-
ments. By the end of this period approximately 88% of the budgeted funds for
the first year have been expended.

On May 2nd the project lost one of its charter participants and
leading forces in the death of Paul M. Fitts. He was, at the time, serving
as Co-Principal investigator. While the loss of his leadership will be
profoundly felt, it is our intention that the program will continue with
substantially the same goals and objectives. Attempts will be made to con-
tinue to pursue the approaches to problems which he so ably represented. Dr.
Pew has been appointed to replace him as Co-Principal investigator to
represent the Human Performance Center in this interdisciplinary program.

Work is continuing on conduct and analysis of experimental studies
of human performance characteristics in manual control tasks and development
of facilities and techniques for on-line analysis of human performance data.

1. EXPERIMENTAL STUDIES

Operator Performance in Three-State Relay Control Systems

A paper entitled "Performance of Human Operators in a Three-State
Relay Control System With and Without Explicit Velocity Information" was
presented by Dr. Pew at the 6th National Symposium on Human Factors in
Electronics which was held in Boston on May 6th-8th, 1965. This paper, which
is included as Appendix A, describes the results of the explicit velocity
display experiment and the major findings of Experiment 65-1 described in the
last status report concerning the use of display blanking to evaluate the
time required to process visual feedback.

A second study employing display blanking (65-4) is currently being
planned to explore the role of signal predictability or coherence in deter-
mining the visual-feedback processing time.

Operator Performance With Predictable Input Signals

Data collection in Experiment 65-2 on sine wave tracking is complete and development of the power spectral analysis program is complete. The first set of analyses of the power spectrum of the operator's velocity error signal (difference between the derivative of the input signal and the derivative of the operator's output) have been completed and compilation of these results is underway.

Data collection has been initiated in the study described in the previous status report which examines the ability to learn to reproduce a precisely specified movement pattern (65-3).

2. RESEARCH FACILITY DEVELOPMENT

Power Spectral Analyzer

The principles and analog computer mechanization of the power spectrum analyzer which has been used in analysis of error data in Experiment 65-2 is described in Appendix B.

Pseudo-Random Noise Generator

As described in a previous report, the noise generator, in the con-ventional configuration, consists of a digital shift register which is pulsed repetitively at a clock frequency, f_c. If each pulse shifts the contents of the register one position to the right, the left-most position is then filled with the logical or of two other positions in the register and if these are selected properly the sequence of states observed in the right-most position repeats only after 2^{n-1} pulses. An analog pseudo-random noise of any desired bandwidth may be obtained by filtering the output of one of the register positions with a filter cutoff frequency f_b.

The empirical evaluation of the output characteristics of this noise generator has focused thus far on describing its output amplitude distribution. Up to now no one has satisfactorily derived the amplitude distribution of the filtered output of such a sequency generator analytically. However, it is possible to argue that the distribution should be Gaussian on intuitive grounds. Assume that the areas between zero crossings of the sequence (transi-tions from "one" to "zero", and vice versa) are independent random variables. Then low pass filtering performs an effective summation of as many random variables as the average number of zero crossings that occur within the memory span of the filter. If the memory span of the filter is long enough, the central limit theorem applies and the filter output should have a distribution which is approximately Gaussian. However, we have observed that for certain combinations of clock frequency and filter bandwidth the time history of the noise generator output appears to be markedly skewed; this has led to the present investigation.

Since the output of the shift register is essentially deterministic and repeats itself after 2^{n-1} states, it is possible to measure the amplitude distribution of the filtered noise output for a particular value of f_c and f_b.

By defining a narrow amplitude "window" and sweeping this window over the range of output amplitudes slowly enough so that a significant percentage of a total cycle of 2^{n-1} states is completed for every amplitude within the window. A continuous plot of the percentage of the total time that the signal spends in every amplitude band is then obtained by averaging the output of a discrete voltage source which has a value +K when the signal is within the amplitude window and zero otherwise. The averaging time constant, window size, and window sweep rate interact with total shift register cycle time and must be adjusted to provide adequate signal sampling and amplitude resolution.

Analysis to date indicates that for the conventional configuration there is an optimum ratio of sequence-generator clock-frequency, f_c, to output filter bandwidth, f_b, of about twenty. For this ratio, the amplitude distribution of the noise is very nearly Gaussian. As f_c/f_b is increased beyond this optimum value the distribution becomes increasingly skewed. For frequency ratios of 80 and above the skewness becomes readily apparent in time history of the noise signal. Large amplitude peaks occur in one direction that have no counterparts in the opposite direction.

As the ratio f_c/f_b drops below the optimum value the distribution degenerates rapidly, so that for a ratio of ten the distribution is not even approximately Gaussian. This is to be expected since for low frequency ratios the effective number of random variables being summed in the filter is not large enough for the central-limit theorem to apply.

The cause of the assymetry of the distribution at high frequency ratios is not fully understood; however, a method for avoiding the problem has been devised. The output of two conventional but shorter shift registers which differ in length by one or two states, may be added modulo two to produce the desired sequence of binary states. This yields a sequence which is very close to maximum length (that is, maximum length for a single shift register of the same total number of states). Preliminary investigation of this method using a 9 stage and 11 stage shift register combination inducates a Gaussian distribution which does not become skewed at high frequency ratios.

Analysis of the noise generator characteristics is continuing and a paper based on these results, containing recommendations for use as a low frequency random signal generator, will be drafted.
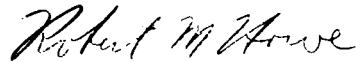
3. RELATED ACTIVITIES

R. W. Pew, R. M. Howe, and J. Herzog attended the 6th Annual Symposium of the Professional Group on Human Factors in Electronics in Boston on May 6th-8th. Pew presented the paper described above which is included in Appendix A.
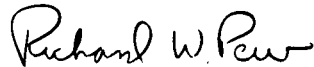
Personnel

The following personnel have worked under this contract during this reporting period.

	Fraction of Time
R. M. Howe	.10
P. M. Fitts	.10
R. W. Pew	.50
J. Duffendack	.40
J. Frait	.50
R. Zauel	.25
L. Kiplinger	1.00
R. Rapley	.50
M. Robb	.50
J. Herzog	.3C

Sincerely yours,

Robert M Howe

Robert M. Howe
Department of Aeronautical and
 Astronautical Engineering

Richard W. Pew

Richard W. Pew
Human Performance Center
Department of Psychology

Co-Principal Investigators

RWP/mr

Performance of Human Operators in a Three-State Relay Control

System With and Without Explicit Velocity Information

Richard W. Pew
Human Performance Center
Department of Psychology
The University of Michigan
Ann Arbor, Michigan

Previous analysis of manually operated two- and three-state relay control systems with inertial dynamics has shown that operators effectively use the velocity information available implicitly in a unidimensional scale of target position to stabilize the system. Pew (1964) demonstrated some ability to represent operators' switching performance in a two-state relay system by use of phase-plane trajectory switching-lines often applied to the engineering analysis of nonlinear systems. The obtained switching lines indicated that target velocity was taken into account in deciding when to switch states. Adams (1965) inferred the use of velocity information from parameter tracking measurements of the best linear representation of operator performance in a three-state system.

The present study was undertaken to extend these results in two directions and to begin a new line of analysis of information processing time in discrete-decision, continuous tracking tasks. First, a three-state system with inertial dynamics was studied to investigate the usefulness of the phase-plane switching-line analysis in the three-state case not previously studied. Second, three display conditions were employed, two of which presented the operator with explicit information about the instantaneous velocity of the target to determine whether provision of such information would produce improved operator performance. Finally, a measure of decision time was derived in the context of this task which makes it possible to evaluate the time required to process feedback information regarding the results of immediately preceding actions.

Method

Description of Task

The three-state relay controller with acceleration dynamics which formed the basis of the operators' task is diagrammed in Figure 1. The operator controlled the position of the target along the horizontal dimension of an oscilloscope by actuation of two piano-like keys that were operated by the index finger of each hand. The pure acceleration dynamics, represented in the frequency domain by k/S^2, were those of an idealized inertial system. Actuation of the left or right keys applied a constant force to this simulated inertia toward the left or right respectively, and produced a constant acceleration in that direction for the duration of actuation. When neither key was active the target coasted with a constant velocity determined by the

state of the system at the termination of the last previous response.
Actuation of both keys simultaneously had the same effect on the system as
when neither key was active. A force of 150 gms over a distance of 0.7 mm
was just sufficient to actuate the microswitch under each key.

The display condition that served as a reference for comparison
with the explicit velocity displays presented the instantaneous position of
the target dot along the horizontal axis of the CRT as is usual with com-
pensatory displays (Displacement Condition: D). Zero error was at the
center of the CRT. In the Velocity Vector Condition (VV) a horizontal line
whose length and direction with respect to the target were directly propor-
tional to instantaneous target velocity was superimposed on the target dot.
A vector one cm in length corresponded to a velocity of two cm/sec.

The display for the Phase-Plane Condition (PP) was two-dimensional
with target position along the horizontal axis and target velocity on the
vertical axis. Since the target was constrained by the dynamics of the
inertial system, it moved along one of two families of parabolic trajectories
concave to the right or left depending on which key was activated. Velocity
to the right was defined to be upward and positive and velocity to the left
was downward and negative with respect to the center of the CRT. As with the
velocity vector presentation one-cm vertical displacement corresponded to a
velocity of two cm/sec.

Subjects were required to return the target to the origin from one
of three initial conditions and to maintain it there for the remainder of a
6.6-sec. trial. The initial conditions were all to the right of the center:
(1) 5.0-cm position error, zero velocity; (2) 5.0-cm position error, 1.95-cm/
sec. velocity to the left; and (3) 3.0-cm position error, 1.98-cm/sec. velo-
city to the right.

Three values of system gain, k, or acceleration constant were
studied having nominal values of 2.0, 10.0, and 30.0 cm/sec^2. Due to an
apparatus malfunction the accelerations applied by actuation of the left and
right keys were not precisely equal. For the left key they were 2.03, 10.32
and 30.16 cm/sec^2 respectively while for the right key they were 2.52, 13.00
and 38.20 cm/sec^2. These differences have been taken into account in any
computations in which they were involved. The differences were small enough
that subjects did not report being aware of them except in the case of two
subjects with the 30-cm/sec^2 acceleration.

Subjects and Procedure

Eighteen University of Michigan undergraduate male juniors and
seniors served as paid subjects. They were divided into three groups so
that six served for a total of eight one-hour daily sessions in each of the
three display conditions.

Subjects sat with their eyes approximately 50 cm from the CRT with
the index finger of each hand resting on the appropriate key. They wore
earphones and listened to moderate intensity white noise to mask the auditory
apparatus cues.

At the beginning of a typical trial the experimenter interrupted the noise in Ss earphones as a signal that two seconds later the target would move instantaneously to the initial condition position and that error scoring would begin. S was to begin responding immediately and to attempt to return the target to the origin. If he maintained the target within the bounds of the CRT the trial terminated after 6.6 sec. and E then informed S of his error score for that trial. If S lost control of the target and it exceeded the limits of the CRT, the trial was automatically terminated and he was arbitrarily assigned a maximum error score of 30 cm-sec. In order to discourage S from anticipating the intial movement of the target, on twenty-five percent of the trials the target did not move and S was verbally reprimanded if he responded on any of these false trials.

The essential features of the instructions to S included a description of the task, an explanation of the meaning of the integrated-absolute-error (IAE) score in terms of the area under the curve describing position error as a function of time, and the instruction that he was to return the target to the origin and hold it there in such a manner that he minimized the IAE he obtained. It can be shown that the minimum-IAE criterion is essentially equivalent to the minimum-time criterion for the conditions under study (Pew, 1963).

Each daily session for each S consisted of 5 consecutive trials under each combination of the three acceleration constants and three initial conditions for a total of 45 trials. The sequence of the nine blocks was randomized over subjects and over sessions for each subject. However, all Ss knew in advance which acceleration and which initial condition would occur during the next block of five trials.

During the first six sessions all Ss practiced with the display condition to which they were assigned. On Days 7 and 8 each group transferred to a new display condition. The displacement group used the velocity-vector display while the phase-plane and velocity-vector groups transferred to the simpler displacement display.

On every trial integrated-absolute-error was computed; target displacement and velocity as a function of time were recorded on a strip chart, and for half the Ss an analog tape recording was obtained of the state of each key as a function of time. This latter record was later analyzed via a digital computer to obtain precise measures of interresponse times.

Results

Error Score Analysis

The integrated-absolute-error scores provided the primary evaluation of the effectiveness of the explicit velocity displays. Figure 2a shows the performance with the three display conditions for each of the three values of system gain or acceleration constant during Sessions 5 and

6, the last two training sessions. The performance score shown on the ordinate is the IAE corrected for differences in minimum IAE obtainable with each value of gain and initial condition by the formula:

$$\text{Performance score} = \frac{\text{Obtained IAE} - \text{Minimum IAE}}{\text{Minimum IAE}}$$

Each data point represents the mean of six $\underline{S}$'s performance on ten trials at each of the three initial conditions.

It appears from the graph that explicit velocity information becomes important only when the system sensitivity or acceleration constant is high. This evaluation was supported by the variance analysis of the last two practice sessions which showed a significant display x acceleration interaction ($p < .05$) but no display main effect. Main effects of acceleration and initial condition were also significant ($p < .01$), as might be expected. A significant display x acceleration x initial condition interaction ($p < .05$) further supported the finding of differential usefulness of the extra velocity information.

Examination of the effect of practice with each display for the three levels of acceleration constant (Figure 3) suggests that it took the phase-plane group one session to become accustomed to the two-dimensional display but thereafter they performed about as well as the velocity-vector group. On the other hand, at the highest acceleration value the displacement display was inferior throughout training.

Figure 2b shows average performance scores before and after each group transferred to the new display condition. Here also means have been accumulated over ten trials for each of six subjects and three initial conditions. Since the velocity-vector (VV) group performance does not change when they begin working with the displacement (D) display but the displacement group shows improvement at the highest acceleration value when they transfer to the velocity-vector display, one may infer that the explicit velocity information is serving as an aid to training rather than as an aid to performance. When the extra information is taken away no decrement results while adding it improves performance. The decrement shown for the phase-plane group could be interpreted as the effect of negative transfer from the two-dimensional to a one-dimensional task. These subjects essentially had to learn a new task when the target no longer moved in two dimensions. Presumably further practice would bring their scores back in line.

Separate analyses of variance were performed for each of the three display groups. For the velocity-vector and phase-plane groups neither a significant session (before and after transfer) main effect nor a session by acceleration interaction was demonstrated ($F < 1$). Evidently the performance decrement shown in Figure 2b for the phase-plane group may be attributable to chance alone. For the displacement group both the session main effect and the session by acceleration interaction are only marginally significant ($p < .10$)

In summary, explicit velocity displays appear to play a role in helping subjects to learn to make use of the implicit velocity information available in the usual compensatory display, particularly when the system sensitivity is high.

From the point of view of potential application, the velocity-vector display appears to have two advantages over the phase-plane presentation. It could be compatible with and easily implemented for a two-dimensional control task while the phase-plane would require separate displays for each dimension. In addition, the learning data suggest that the velocity-vector display has an inherent compatibility with the controlling task which reduces the time required for familiarization, at least for the naive subjects used in this study.

Phase-Plane Switching Point Analysis

One reason for studying the effects of three initial conditions was to provide data for further examination of the locus of switching points chosen by subjects in their attempts to null out the initial error. Figure 4 shows the mean switching points plus or minus one standard deviation for two subjects for each combination of initial condition and acceleration value. The subject shown in Figure 4a used the phase-plane display while the subject in Figure 4b served in the velocity-vector group. Each switching point was determined from the mean of ten observations. Hence these phase-plane trajectories may be regarded as representing the subject's average transient performance for each initial condition--acceleration combination. It may be seen that the subject initiated his first response at the initial conditions indicated by the dots in the right hand two quadrants of each figure. He continued to hold the left key down until the conditions of velocity and position associated with the first switching point were reached. In every case there is then a brief period when either both keys were released or both keys were depressed and then the final segment of the trajectory shown corresponds to right-key activation. These trajectories were terminated arbitrarily at the zero-velocity axis since this analysis extended only through the first switching point.

It is evident from Figure 4 that the attempt to provide a range of possible switching points by varying the initial conditions was only marginally successful. The first segment of each set of the three trajectories are too close together. Nevertheless, as shown in Figure 4a Subj: NM, using the phase-plane display, came very close to placing all of his mean switching points on the time-minimum optimum trajectory. Subj: DD, using the displacement display, was more typical of the other subjects whose data was analyzed in this way in that his switching locus was not easily characterized. However, as shown for DD, most subjects tended to overshoot the origin and most exhibited surprisingly little variability over trials in their choice of switching points. The obtained average switching performance was examined for systematic differences which could be attributed to differences in the display group to which subjects were assigned, but no systematic differences were observed.

One general finding of this analysis was that most Ss, when operating with acceleration constant equal to 30 cm/sec^2, failed to make

use of the maximum velocity capability of the system. Instead they tended
to follow the pattern: accelerate-coast-decelerate. Some coasting is shown
in Figure 4 but for most other subjects it was more pronounced. A minimum-
time optimal controller would not coast. However, if we accept the operator's
inherent variability in locating the desired switching point precisely in
time, then for a very sensitive system there is a trade-off between the
relative cost of a switching-time error and the relative cost of limiting
velocity to a value less than the maximum available. It appears that this
trade-off was resolved in favor of limited velocity when the velocities were
in the range where a 50-ms timing error produced a position error of 1/2 cm.

Feedback Processing Time Analysis

As learning of the task progressed over the six sessions of train-
ing, most subjects developed the strategy of nulling out the initial error
with two or three carefully timed responses and then shifting to a pulsed
mode of responding. Each pulse introduced a discrete change in velocity and
this mode effectively reduced the order of the system from acceleration
control to velocity control.

For purposes of analysis, pulses were arbitrarily defined as
responses whose total duration was shorter than 120 ms. For responses this
short it could be argued that pulse preprogramming had occurred, that is,
Ss did not modify the planned pulse duration while the pulse was in progress.
Consider for a moment that a subject has just executed a preprogrammed pulse.
He now has three alternative actions available: (1) The pulse produced a
velocity change insufficient to compensate for the existing error and an
additional pulse with the same key is required. (2) The velocity change
overcompensated and a pulse with the alternate key is required or (3) The
pulse was successful in bringing the target inperceptibly near the origin
with no residual velocity and, for the moment, no further response is
required.

Since the original pulse was preprogrammed, the time required to
reach decision (1) or (2) must be included in the pause after the pulse and
before the next response. The only information on which to base such a
decision is either that presented visually or that derived from the feel of
the keys. Alternatively the subject may program two pulses in advance to
be separated by a specified amount of time and rely on no feedback about the
result of the last response. Thus with the exception of the latter explana-
tion which will be dealt with subsequently, the time between responses
provides a measure of the time needed to process feedback about an on-going
response activity. It is different from a discrete reaction time measurement
in several ways. First, the information on which the reaction is based is
ill-defined. It depends on a subtle comparison of the position and velocity
predicted and achieved on the last response. Second, it is a reaction which
is almost completely contingent on the immediate past history of the subject's
performance. Third, it is a reaction that must be smoothly integrated into
an on-going stream of activity.

To provide a measure of this feedback processing time, a digital
computer analysis of the data describing the sequential states of the keys

as a function of time was performed to obtain the distribution of response times following pulse responses (shorter than 120 ms) for about half of the group of 18 subjects. By the sixth session all but one of them were pulsing regularly. Two typical distributions are shown in Figure 5. The mean pause or response time has been plotted separately for responses with the same and alternate hands. Each histogram contains the accumulation of pulses for that subject over the first six sessions since close examination of the individual session data revealed no systematic change in the distribution with practice. Although it may be seen that there are differences in the proportion of same and alternate key responses generated by the two subjects, normalizing those absolute distributions reveals that their shapes and locations are very similar. For every subject the mode of the distribution of responses with the same key appeared with less delay than the mode of the distribution for responses with the alternate key. This is inconsistent with the psychological data suggesting a refractoriness to response repetition, but is consistent with Bertelson's (1961) finding of a repetition enhancement effect in serial-reaction-time studies.

In addition to the interesting interpretation of these data in the framework of discrete reaction time studies, it is tempting to propose also that they are of interest for the specification of sampling rates in sampled data models of the sort described in Young and Stark (1965). If so, these data argue strongly for variable-rate sampling and provide a first step in the direction of specifying what the distribution of sampling intervals should be. Although the information on system velocity and position at the end of each pulse was not available for analysis, it is anticipated that the specific sampling time taken by subjects may be functionally related to these variables, making it possible to predict sampling rates on the basis of measurable task variables.

In order to examine in more detail the timing of the decision processes underlying performance with the pulsed-mode in this relay control system one further exploratory study has been completed. Four of the subjects who served in the main experiment returned for several additional sessions in which a new variable was introduced. Whenever the subject made a pulse response shorter than 120 ms, the visual display was blanked out for a predetermined period of time ranging from 177 to 410 ms. This blanked period could begin immediately with the termination of the pulse or could be delayed up to 335 ms following the pulse. For this study only one initial condition (3-cm position error, 2.03-cm/sec. velocity to the right) and one acceleration value (30 cm/sec^2) were used. Furthermore, Ss were encouraged to pulse. The distribution of response times for the twelve combinations of delay and blanking studied are shown in Figure 7 for Subj: RS. The other three subjects were performing so well that they needed to make pulsing corrections less frequently. Since only interresponse times following pulses were analyzed, these Ss failed to provide enough data to produce well-defined distributions.

The fine structure of these distributions may be of some interest but the main finding which systematically characterizes these distributions is shown in Figure 7. When blanking is introduced, the overall distributions shown in Figure 6 are effectively decomposed into two modes. The first mode

to appear has a position in time that is fixed with respect to the termination of the pulse. No matter what the delay and duration of blanking the position of this first mode is relatively fixed. The time delay associated with this mode must either represent a delay associated with other sources of feedback or, more likely, a preprogrammed time delay such that a second response is executed regardless of the consequences of the first one. On the other hand, as blanking is extended, a second mode to the distribution appears which varys rather systematically with the termination of blanking. The responses contributing to this mode appear to be intimately tied to the return of visual information to the display. The intercept or average delay associated with this mode is about 320 ms for the alternate key responses and about 260 ms for the same key responses. These figures represent the best estimates obtainable from these data for the modal time necessary to process visual feedback for this task.

As the blanking is systematically delayed, a larger and larger proportion of the responses appear in the first mode. From this data on one subject it appears that at least 270 ms delay is necessary before much relevant information can be extracted from the display prior to blanking. This is consistent with the 300 ms delay in responding associated with the return of visual information. Further studies involving display blanking are planned to see if other subjects behave in a similar manner when they are at a stage of learning conducive to frequent pulsing and to see if the variable of input predictability can be systematically manipulated. This line of analysis shows considerable promise for providing a bridge between discrete-reaction-time studies and continuous-control system investigations.

Summary

This study has focused attention on the kinds of analysis that can be employed with the highly specialized relay controller in order to promote further understanding of the underlying control processes utilized in continuous-control tasks. Display manipulation showed the role played by explicit velocity information in the acquisition of high levels of performance. The phase-plane analysis showed the possibility of a meaningful representation of a subject's transient performance in nulling out an initial condition although further work will be necessary before this analysis will produce many useful generalizations. Finally the measurement and manipulation of the time necessary to process feedback information has many potential implications for bringing discrete reaction time data to bear on continuous-control behavior and for the representation of an operator as a variable-rate sampling system.

References

Bergeron, H. P., Kincaid, J. K., & Adams, J. J. Measured human transfer functions in simulated single-degree-of-freedom nonlinear control systems. NASA Technical Note D-2569, January, 1965.

Bertelson, P. Sequential redundancy and speed in a serial two-choice responding task. Quart. J. exp. Psychol., 1961, 12, 90-102.

Pew, R. W. Temporal organization in skilled performance. Ph. D. thesis, University of Michigan, 1963.

Pew, R. W. A model of human controller performance in a relay control system. Proc. 5th National Symposium on Human Factors in Electronics, San Diego, California, May, 1964.

Young, L. R., & Stark, L. Biological control systems--A critical review and evaluation. Developments in manual control. NASA Contractor Report CR-190, March, 1965.
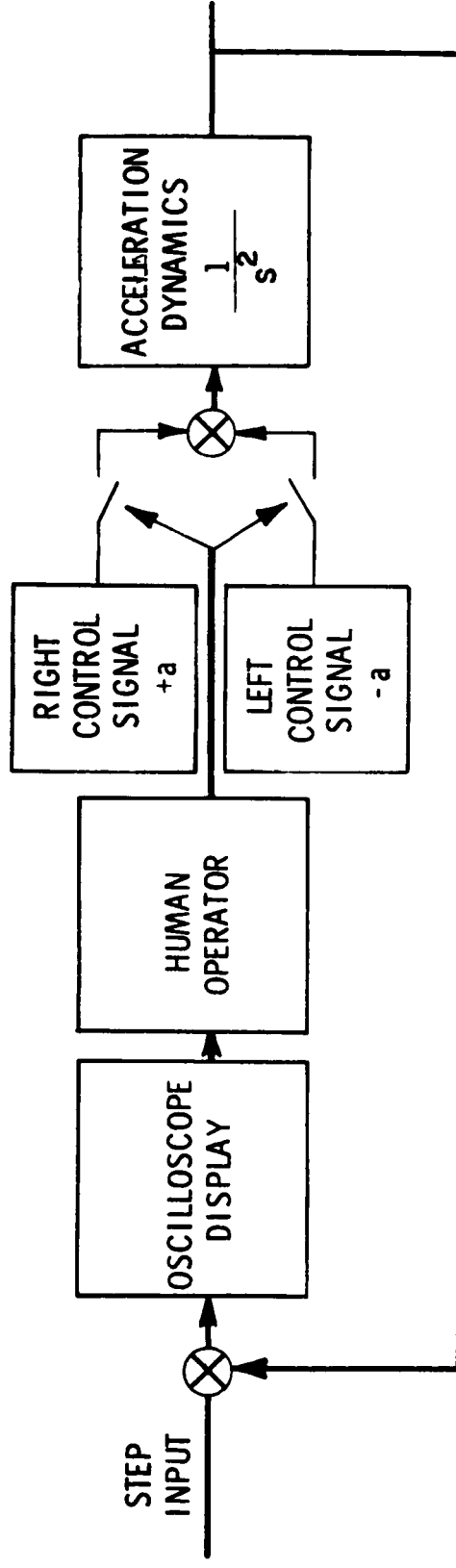
Figure 1   Block diagram of manually-operated relay control system
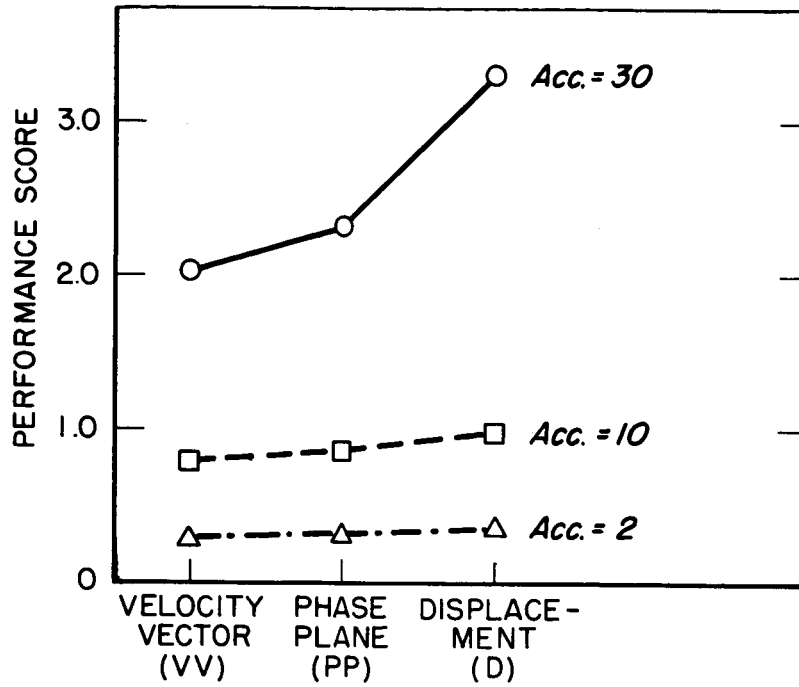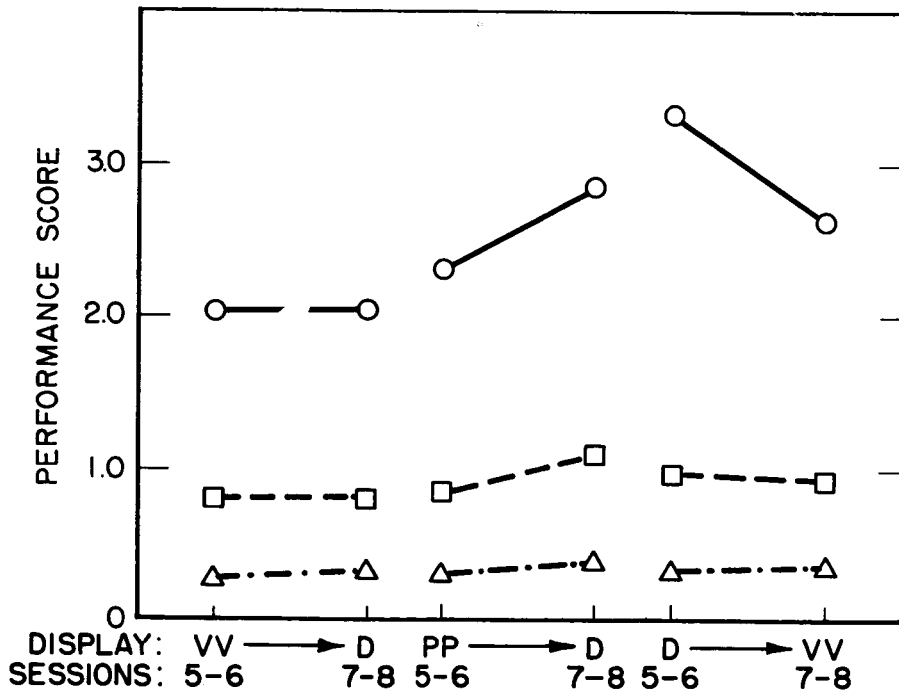
Figure 2   (a) Performance score of subjects in three display conditions for the three values of acceleration constant. (b) Performance before and after transfer to a new display condition for the three values of acceleration constant
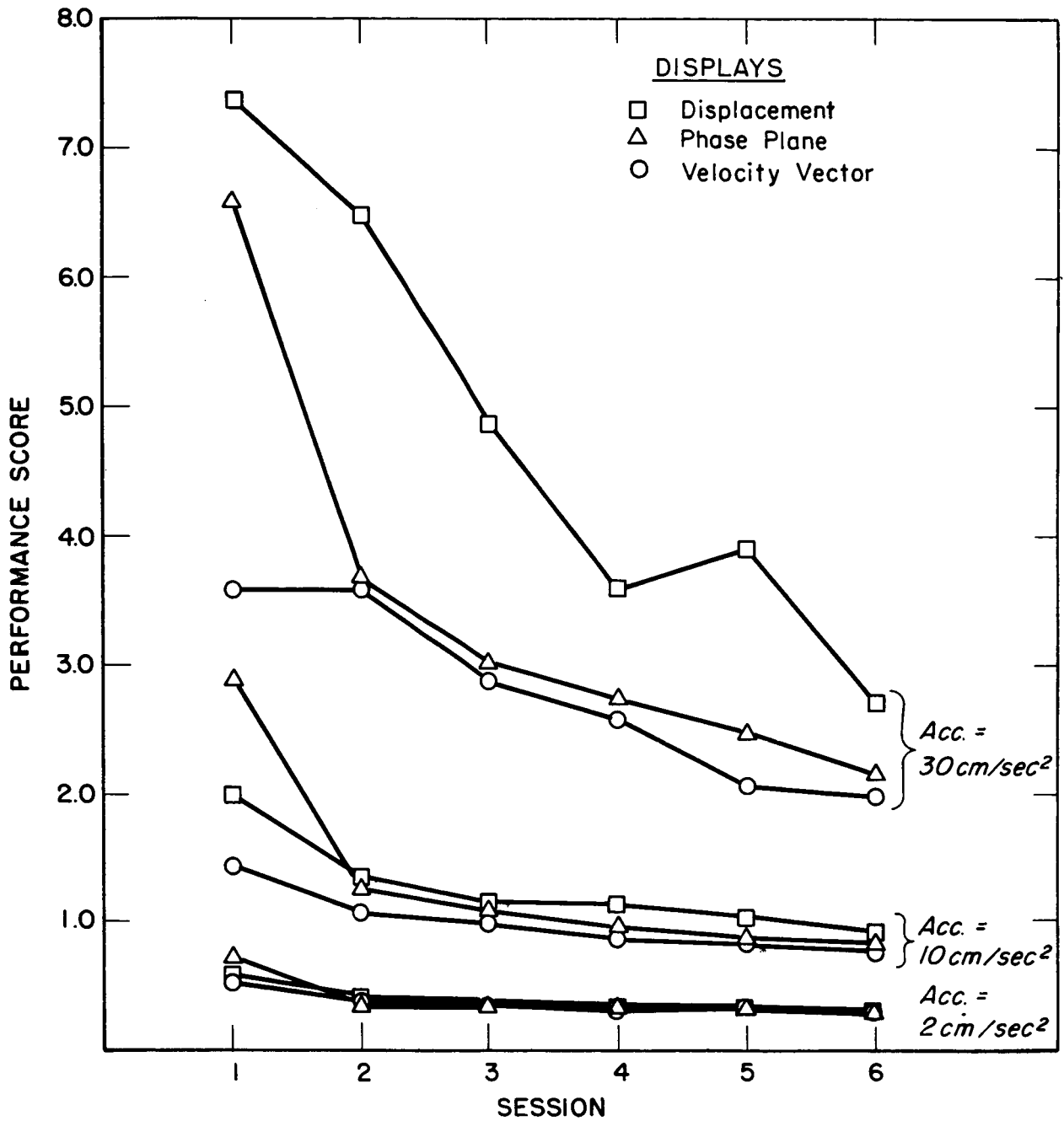
Figure 3   Performance score as a function of daily sessions of practice for each display group and each acceleration constant
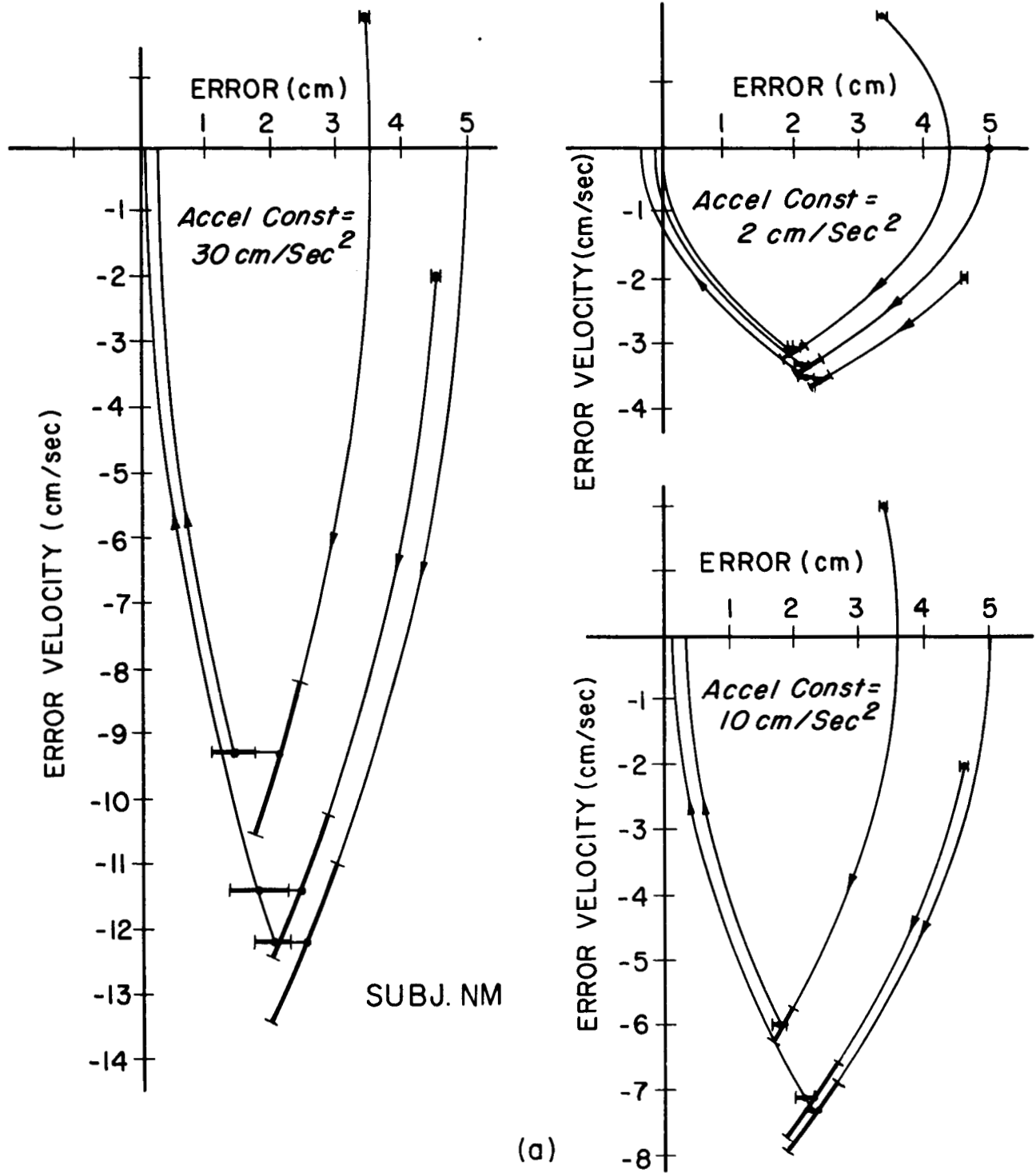
Figure 4   Average phase-plane trajectories for all combinations
                  of acceleration constants and initial conditions show-
                  ing mean switching points and ±1 σ about the mean
                  switching points. (a) Data for Subject: NM. (b) Data
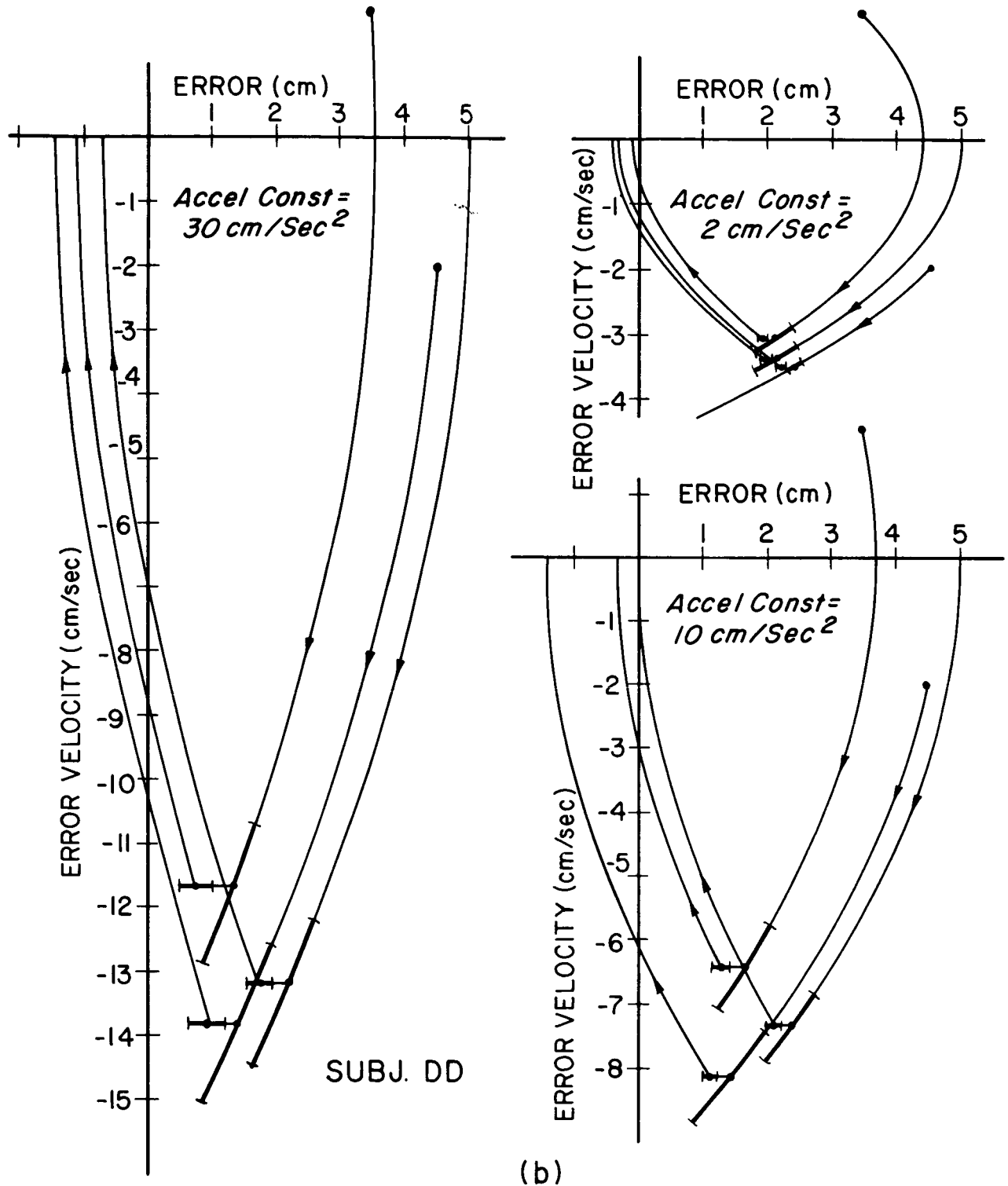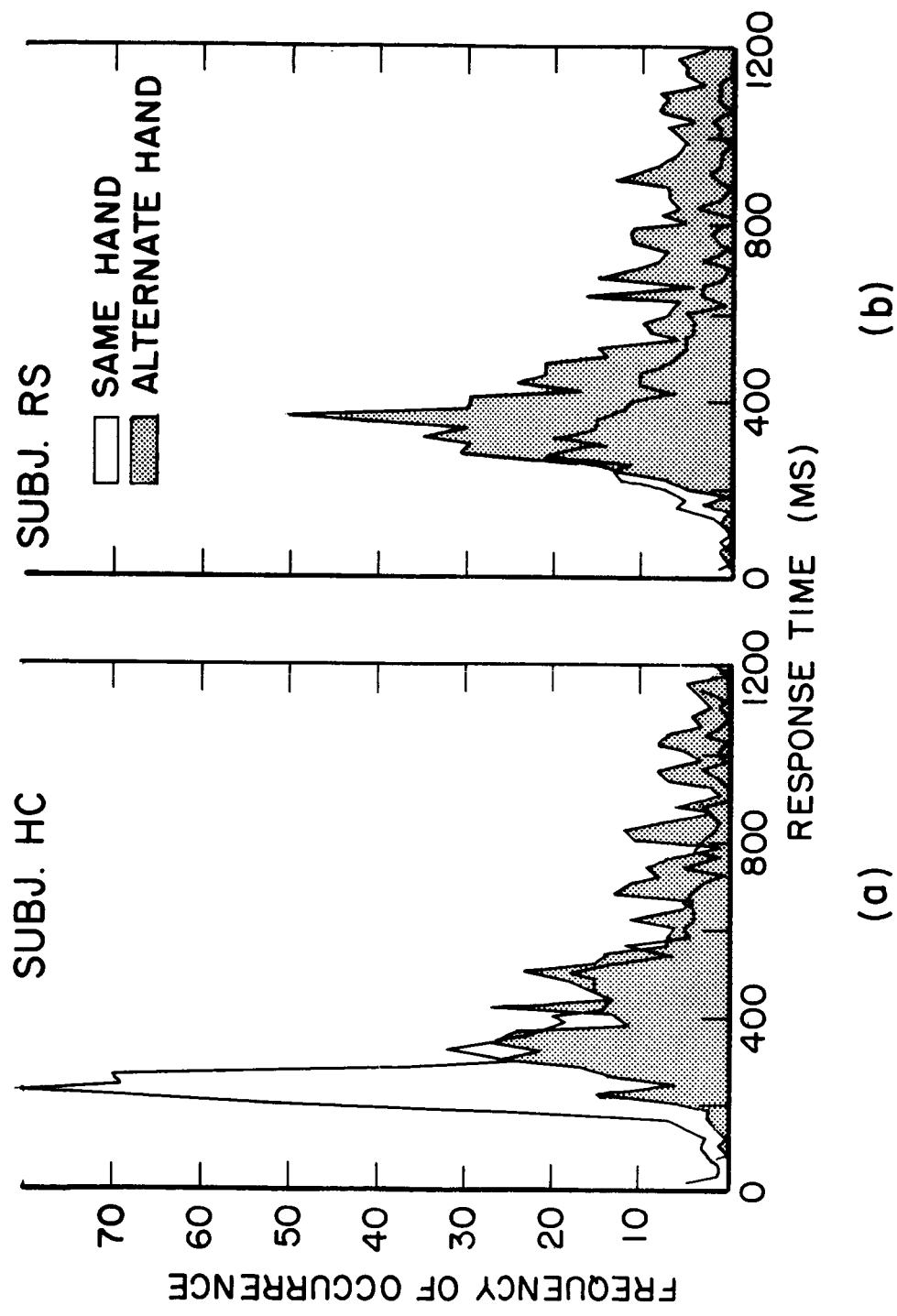   for Subject: DD.

Figure 4 (Con't)

Figure 5   Distribution of interresponse times following pulse
responses for the cases in which the subsequent response
was made with the same or alternate hands. (a) Data for
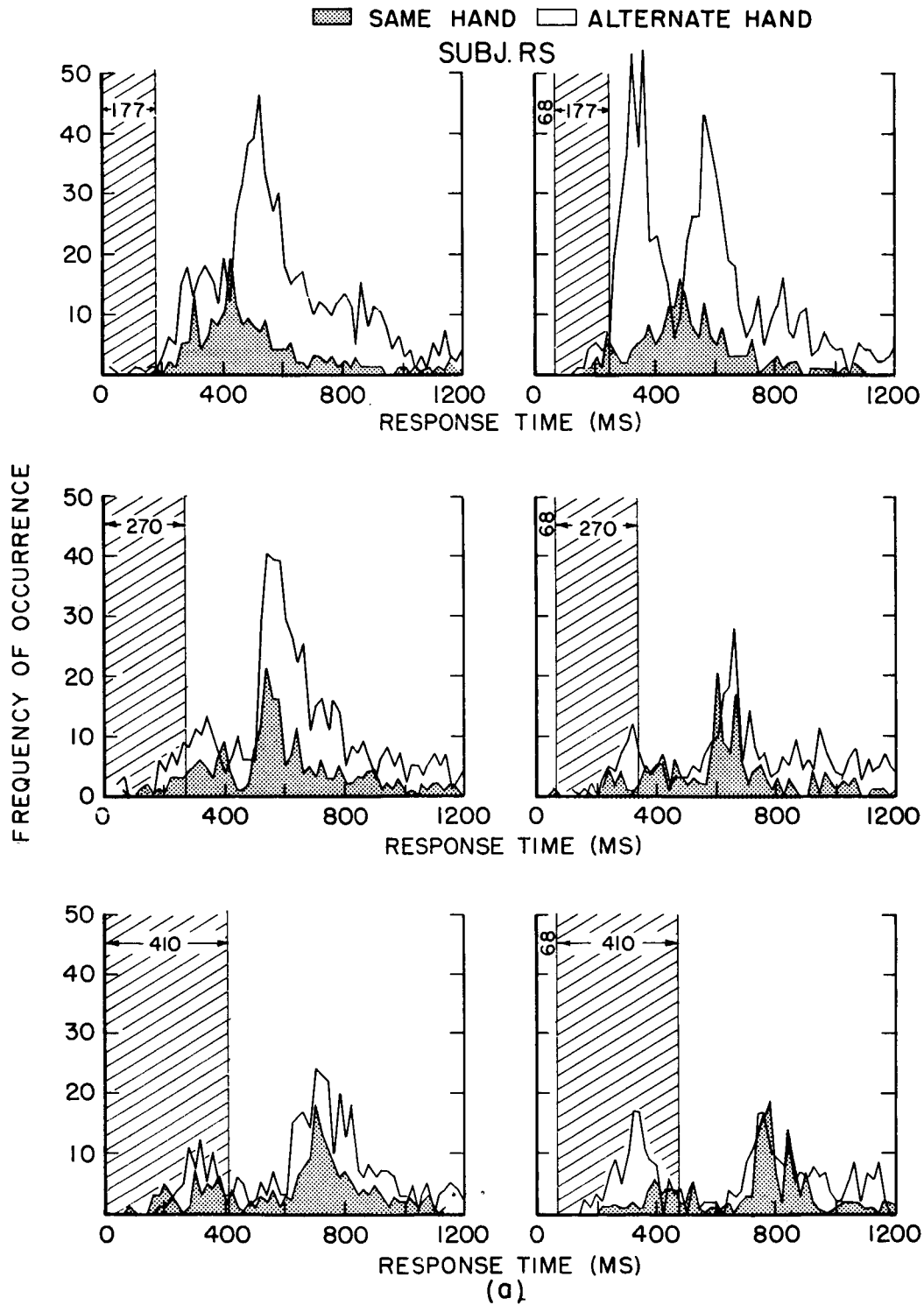Subject: HC. (b) Data for Subject: RS.

SAME HAND ☐ ALTERNATE HAND

Figure 6   Effect of display blanking on the distribution of inter-
response times following pulse responses for cases in
which the subsequent response was made with the same or
alternate hands. Shaded area indicates the period of
time for which the display was blanked. Durations given
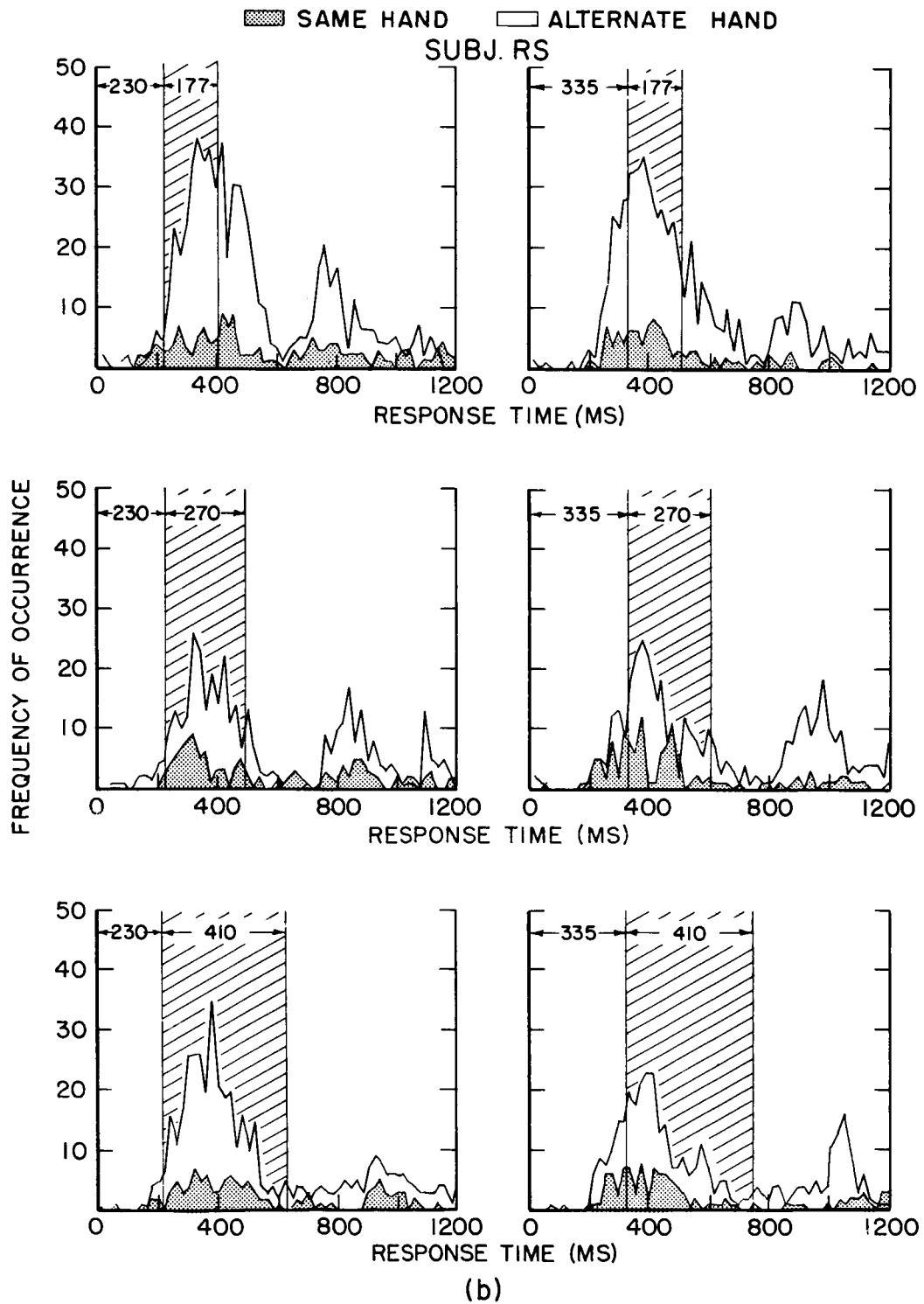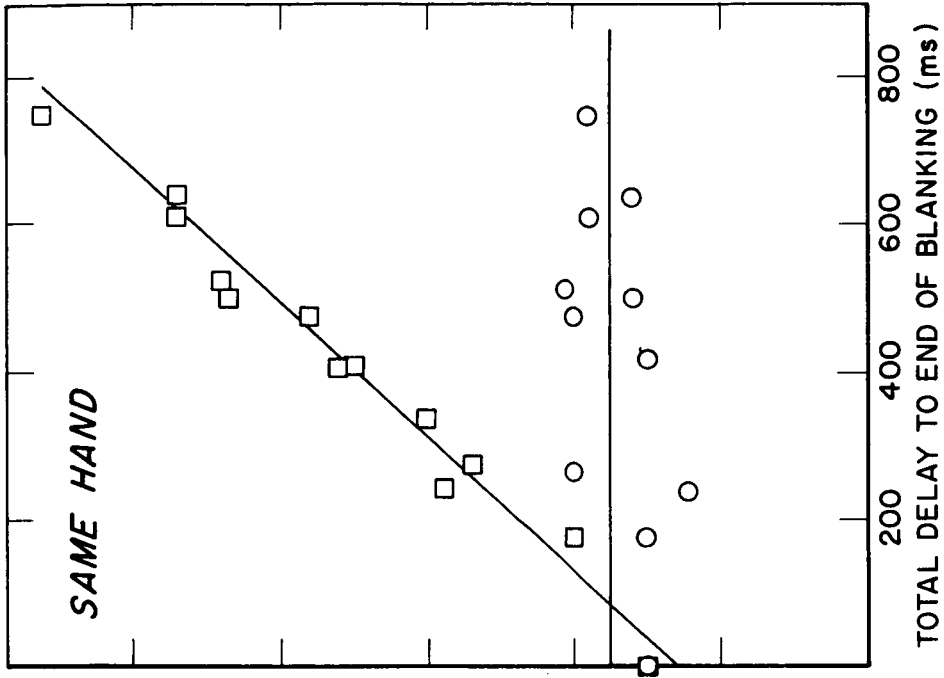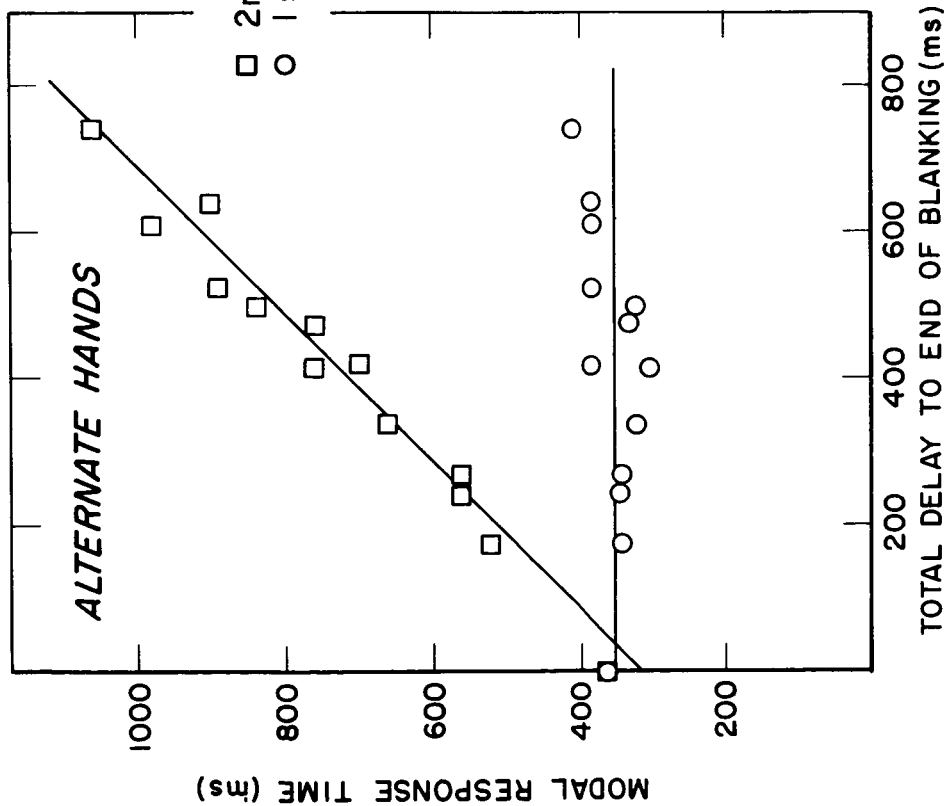are in milliseconds.

Figure 6 (Con't)

Figure 7   Modal interresponse times as a function of the time at which blanking terminates, showing the two modes of the distributions characteristic of the data of Figure 6.
(a) Data for pairs of responses with alternate hand.
(b) Data for pairs of responses with same hand.

Appendix B

Analog Computation of Power Spectra

John C. Duffendack

I. Introduction

The measurement of power spectra by either digital or analog tech-
niques has been accomplished more or less routinely for a number of years.
However, research workers who have reason to use power spectral measurements
of this sort are often not themselves electrical engineers or computer experts.
The description that follows is intended to provide a sufficiently detailed
explanation of the method so that individuals with access to an analog computer
may make use of the technique, with a minimum of technical consultation.

The development of this particular analog implementation was under-
taken in order to analyze the error signal obtained when human operators are
attempting to track a purely sinusoidal signal. Other mechanizations are
possible such as computation and transformation of correlation functions.
However, the input signals to the system under study were sinusoidal and a
relatively narrow band of power in the error signal was aniticipated so that a
straight forward method based on a set of parallel, narrow-band filters was
chosen. This implementation has the advantage of requiring only a single pass
through the data and is equally suitable for on-line or off-line analysis. As
described, the system requires six operational amplifiers and one electronic
multiplier for each filter employed.

II. Theory

Spectral densities are generally defined in terms of integrals over
time with doubly infinite limits. However, the practical measurement problem
must necessarily be concerned with functions measured over a finite interval
of time. It is only possible to approximate asymptotically the infinite time-
average spectral density.

Given the function, $f(t)$, it is desired to approximate the power
spectral density function, $\Phi(\omega)$, i.e., the power per unit bandwidth associated
with $f(t)$ at each frequency, ω. The power spectral density is usually defined
as the fourier transform of the autocorrelation of $f(t)$. Since this dis-
cussion is concerned with the direct measurement of spectral density we will
define $\Phi(\omega)$ in a more direct fashion. Many authors define the power spectral
density as

$$\Phi(\omega) = \frac{1}{2\pi} \lim_{T \to \infty} \frac{\left| \int_{-T}^{T} f(t)\, e^{-j\omega t}\, dt \right|^2}{T} .$$

Unfortunately, this definition is not mathematically justified and fails
occasionally as outlined by Davenport and Root (1958). For direct measure-

ment, as proposed here, an appropriate definition is given by Bekey (1962). He defines the spectral density function as a double limit as $\Delta\omega$ and T approach zero and infinity respectively.

$$\Phi(\omega_c) = \lim_{\Delta\omega \to 0} \lim_{T \to \infty} \frac{\int_{\omega_c - \frac{\Delta\omega}{2}}^{\omega_c + \frac{\Delta\omega}{2}} \frac{\left|\int_{-T}^{T} f(t)\, e^{-j\omega t}\, dt\right|^2}{T}\, d\omega}{\Delta\omega}. \quad (1)$$

The integral over ω in the above equation represents the average power in a signal of duration 2T for a range of frequencies of width $\Delta\omega$ centered about the frequency ω_c. Implicit here is the assumption that f(t) is ergodic.

This function $\Phi(\omega)$ may be represented at a given number of points as the output of a series of filters with appropriate squaring and averaging devices as shown in Figure 1.
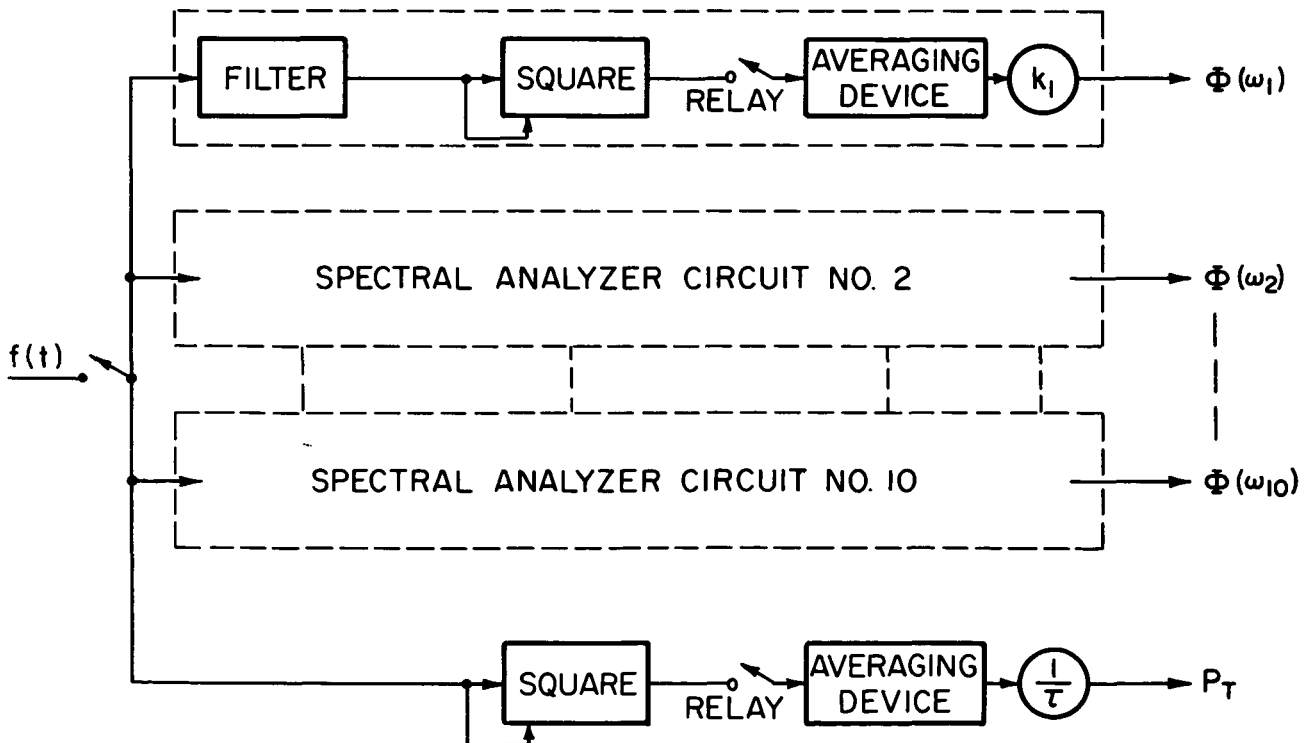

Figure 1. Block Diagram of Analog Spectral Analyzer

Each filter passes the power within its pass-band and the output of each averaging device is proportional to the effective averaging time (τ) and the filter bandwidth (B_i) as well as the signal characteristics. It is desirable to normalize $\Phi(\omega)$ such that there is unity area under the spectral density function. Thus, the normalizing constant,

$$k_i = \frac{1}{P_T B_i \tau} \tag{2}$$

is defined where P_T is the total power or mean squared value of $f(t)$. That is, using an integrator for the averaging device

$$P_T = \frac{1}{T} \int_0^T f(t)^2 \, dt \tag{3}$$

and the bandwidth is given by

$$B_i = \frac{\int_0^\infty H(\omega_i) \, d\omega}{H(\omega_i)_{max}} \tag{4}$$

where $H(\omega_i)$ is the filter power gain function. Note that a filter with a rectangular gain function over a bandpass B cycles wide and $H(\omega_i)_{max}$ high would have the same area under the $H(\omega_i)$ curve as the filter described in the the above equation.

Whenever power spectra are estimated from signals over a finite run length, the estimate is subject to statistical variability. When the measurements are obtained from human operators, the run length must be chosen as a compromise between the acceptable range of statistical fluctuation in the measurement and the duration of a run over which the operators behavior may be regarded as stationary in a statistical sense. The choice of filter bandwidth involves a trade-off between statistical variability and the precision with which the frequency components in the power spectrum may be resolved. These trade-offs are reflected in the definition of the expected mean square error of measurement or variance, σ_Φ^2 in $\Phi(\omega)$. The equation definining σ_Φ^2 which is given below assumes that the amplitude distribution of the signal being analyzed is Gaussian; however, the assumption does not appear to be a critical one. Valid approximations may be obtained even when significant departures from normality are observed.

$$\sigma_\Phi^2 = \frac{\Phi(\omega_i)^2}{B_i \tau} \tag{5}$$

where τ, the effective averaging time, is defined as

$$\tau = \frac{1}{\int_0^\infty k(t)^2 \, dt},$$ (6)

and k(t) is the impulse response of the averaging device (for an integrator τ is equal to the integrating time T). For the purpose of estimating σ_ϕ, a new equivalent filter bandwidth is defined as

$$\bar{B} = \frac{\left[\int_0^\infty H(\omega) \, d\omega\right]^2}{\int_0^\infty H(\omega)^2 \, d\omega}.$$ (7)

Note that as the bandwidth or the averaging time gets larger, the rms statistical error σ_ϕ is reduced. However, the trade-off is slow since σ_ϕ varies with $[\bar{B}\tau]^{-1/2}$.

This definition of σ_ϕ may be interpreted as the standard error of estimate in the usual statistical sense. Once $\Phi(\omega_i)$ and $\sigma(\omega_i)$ are known, a 95% confidence interval corresponding to $\pm 2\sigma$ will define the expected variability of the measurement.

The above discussion implies that the analysis of spectral density measurement is to be applied to a single continuous function. The spectral density of several similar runs, however, may be averaged together to reduce the expected data variability assuming that the data are generated by a stationary process. Note that the expected standard deviation $\sigma(\omega_i)$ is reduced from the value for a single run by the fact $n^{-1/2}$ where n is the number of runs of equal time that are averaged.

III. Filter Realization

A large variety of filter types have been used in spectral measurements varing in complexity and cut-off characteristics. A second-order bandpass filter was chosen here for ease of operation and mechanization.

This filter has a transfer function;

$$Y(s) = \frac{s}{s^2 + 2\xi \omega_n + \omega_n^2}.$$ (8)
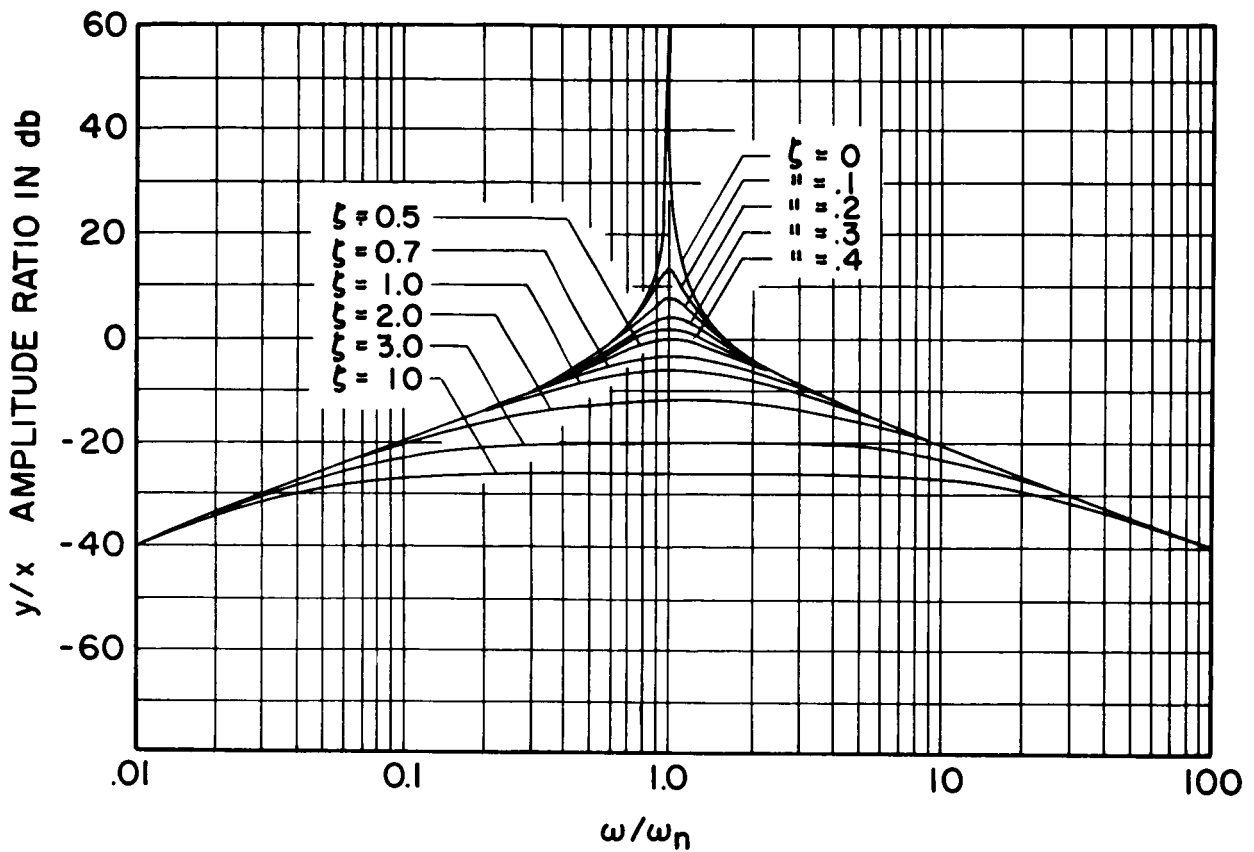
The frequency response of the filter is shown in Figure 2.

Figure 2. Response of Filter to Sinusoidal Inputs

The power gain function $H(\omega)$ may be written as,

$$H(\omega) = \left| Y(j\omega) \right|^2 = \frac{\left(\frac{\omega}{\omega_n}\right)^2}{\left[1 - \left(\frac{\omega}{\omega_n}\right)^2\right]^2 + \left[\frac{2\xi\omega}{\omega_n}\right]^2} \qquad (9)$$

and the maximum power gain is given by,

$$H(\omega)_{max} = \frac{1}{2\xi\ \omega_n} . \qquad (10)$$

The filter bandwidths may be determined by integrating the proper function of $H(\omega)$. From Equation 4,

$$B(\omega_i) = \pi\ \xi_i\ \omega_i \qquad (11)$$

and from Equation 7,

$$\overline{B}(\omega_i) = \frac{\pi}{2} \xi_i \, \omega_i. \tag{12}$$

The expected standard deviation σ_i is then given by,

$$\sigma(\omega_i) = \Phi(\omega_i) \left[\frac{2}{\pi \, \xi_i \, \omega_i \, T} \right]^{1/2} \tag{13}$$

and in terms of decibels, Equation 13 becomes

$$\sigma_{db} \, (\omega_i) = 10 \, \log \left[1 \pm \left[\frac{2}{\pi \, \xi_i \, \omega_i \, T} \right]^{1/2} \right] \tag{14}$$

There are many ways to realize the transfer function of Equation 8, both actively and passively. An active implementation using three operational amplifiers was chosen (see Figure 3). A simpler one-amplifier circuit (see Figure 4) could be used with equivalent results although component selection (values of resisters and capaciters) with this scheme is more difficult.
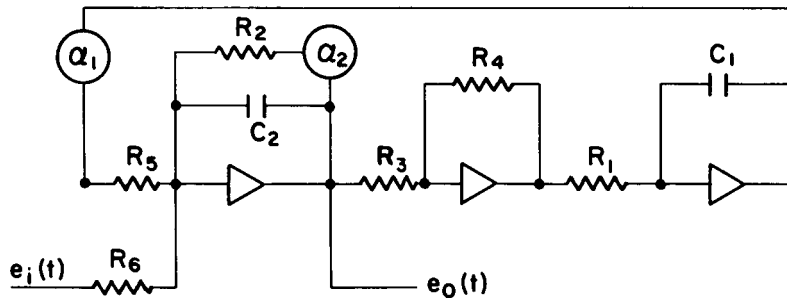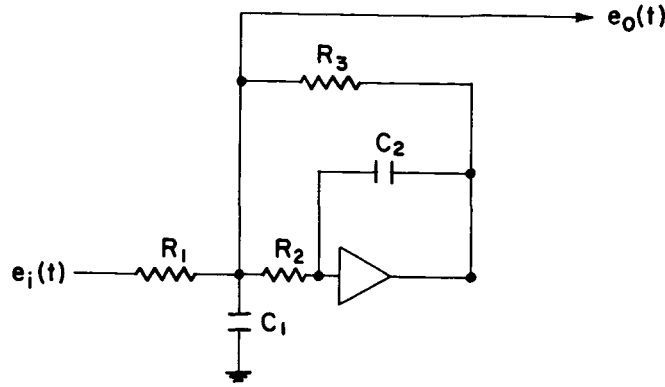

$$Y(s) = \frac{-k \, s}{s^2 + 2\xi \, \omega_n + \omega_n^2}$$

$$k = \frac{1}{C_2 \, R_4}$$

$$\omega_n^2 = \frac{\alpha_1 \, R_4}{C_1 \, C_2 \, R_3 \, R_5 \, R_1}$$

$$\xi = \frac{\alpha_2}{C_2 \, R_2} \quad \frac{1}{2\omega_n}$$

Figure 3. Circuit Diagram and Related Equations for a Three Amplifier, Second Order, Bandpass Filter

$$Y(s) = \frac{+ k \, s}{\dfrac{s^2}{\omega_n^2} + 2\xi \dfrac{s}{\omega_n} + 1}$$

$$\omega^2 = \frac{1}{R_2 \, R_3 \, C_1 \, C_2}$$

$$\xi = \frac{1}{2\omega_n} \frac{1}{C_1} \left(\frac{1}{R_1} + \frac{1}{R_2} + \frac{1}{R_3} \right)$$

$$k = \frac{R_3 \, R_2 \, C_2}{R_1}$$

Figure 4. Circuit Diagram and Related Equations for a One Amplifier, Second
Order, Bandpass Filter

Note that both circuits are simply the realization of a second-order system where the output is taken as the derivative of the usual output (i.e., "back up" one integration).

IV. Selection of Filter Characteristics

There are a number of trade-offs in the actual characteristics of the individual filter which are dependent on the expected properties of the signal to be analyzed and the analog equipment available. The signal frequencies (or at least the interesting parts of it) should be sampled along the frequency axis such that a roughly continuous approximation to $\phi(\omega)$ may be determined. A proper damping ratio should be chosen to give a short filter transient time and small $\sigma(\omega_i)$ while still maintaining a narrow enough bandwidth for proper frequency discrimination (see Figure 2 and Equation 4). The damping ratio may be the same for all filters or varied from filter to filter to decrease $\sigma(\omega_i)$ or increase the filter discriminability. That is ξ_i could be increased in the low frequency filters to increase $\overline{B}(\omega_i)$ and thus sacrifice discriminability for a low $\sigma(\omega_i)$ (see Equation 13 and Figure 5).
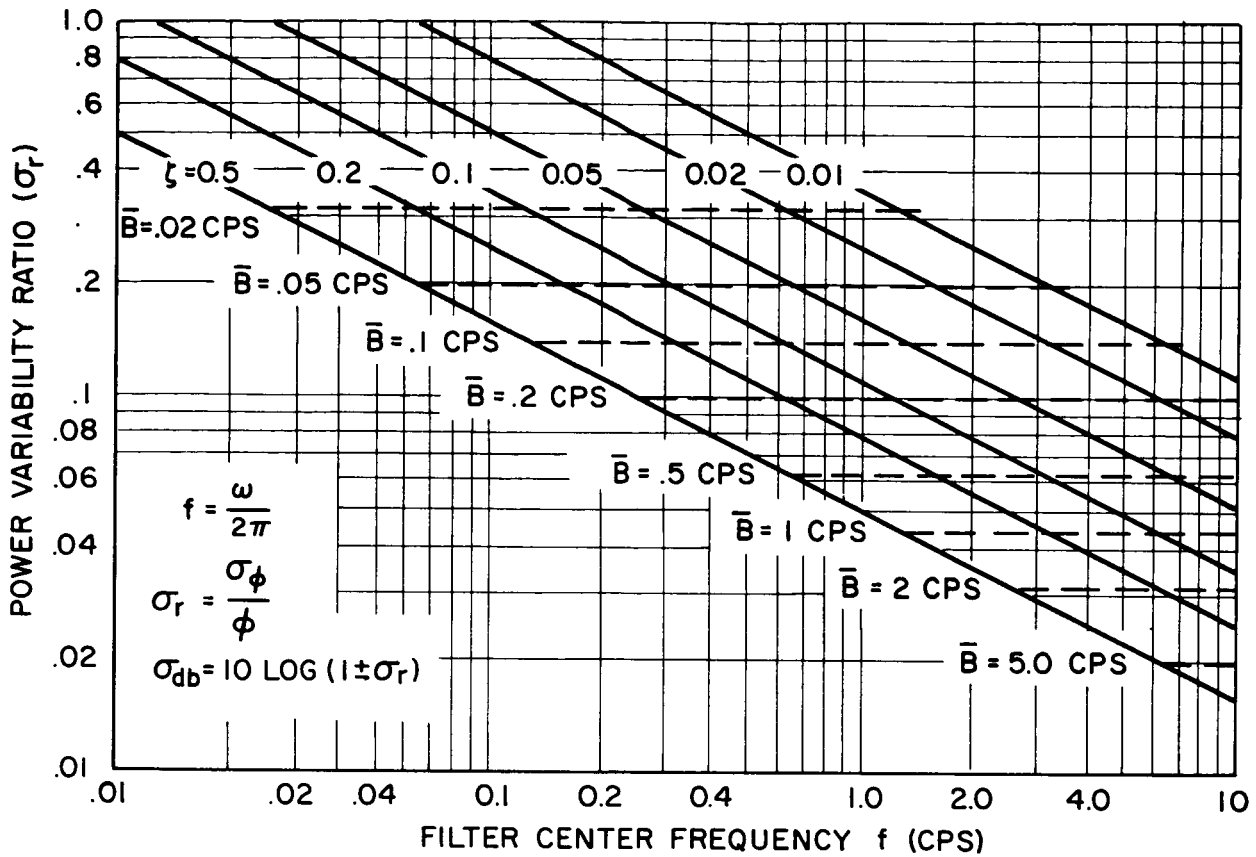
Figure 5. Expected Power Variability for a Run of 80 Seconds

For the band-limited human operator tracking a variety of sinusoidal inputs, during 120 second runs, the following filter characteristics were chosen*:

	$\xi = 0.1$ for All Filters				
ω_1	=	.087 cps	ω_6	=	.803 cps
ω_2	=	.135 cps	ω_7	=	1.25 cps
ω_3	=	.211 cps	ω_8	=	1.95 cps
ω_4	=	.330 cps	ω_9	=	3.04 cps
ω_5	=	.515 cps	ω_{10}	=	4.75 cps

---

*For actual operation these values along with the pre-recorded signal were time scaled up by a factor of 4.

V. Computer Utilization

A 90-amplifier logic controlled analog computer was used for the
spectral analyzer. Pre-recorded signals, scaled up in time by a factor of
four, were fed to the computer from an Ampex SP 300 AM-FM Magnetic Tape
Recorder. A series of relays and timers controlled the automatic analysis
of each run. At the first zero-crossing of the subjects recorded output,
the filters were placed into the operate mode (inputs connected to the inte-
grators). Following this a 6 second delay (24 seconds real time) occurred
to eliminate filter transients. The inputs to the averaging integrators
were then connected and at the end of a 20 second run (80 seconds real time)
the computer was placed in the hold mode while the outputs of the averaging
integrators were read. The computer was manually reset and the process
repeated for the next set of data.

Figure 6 shows one of the ten filter, square and average circuits
set up on the computer. Pots 1 and 2 were used to adjust the filter char-
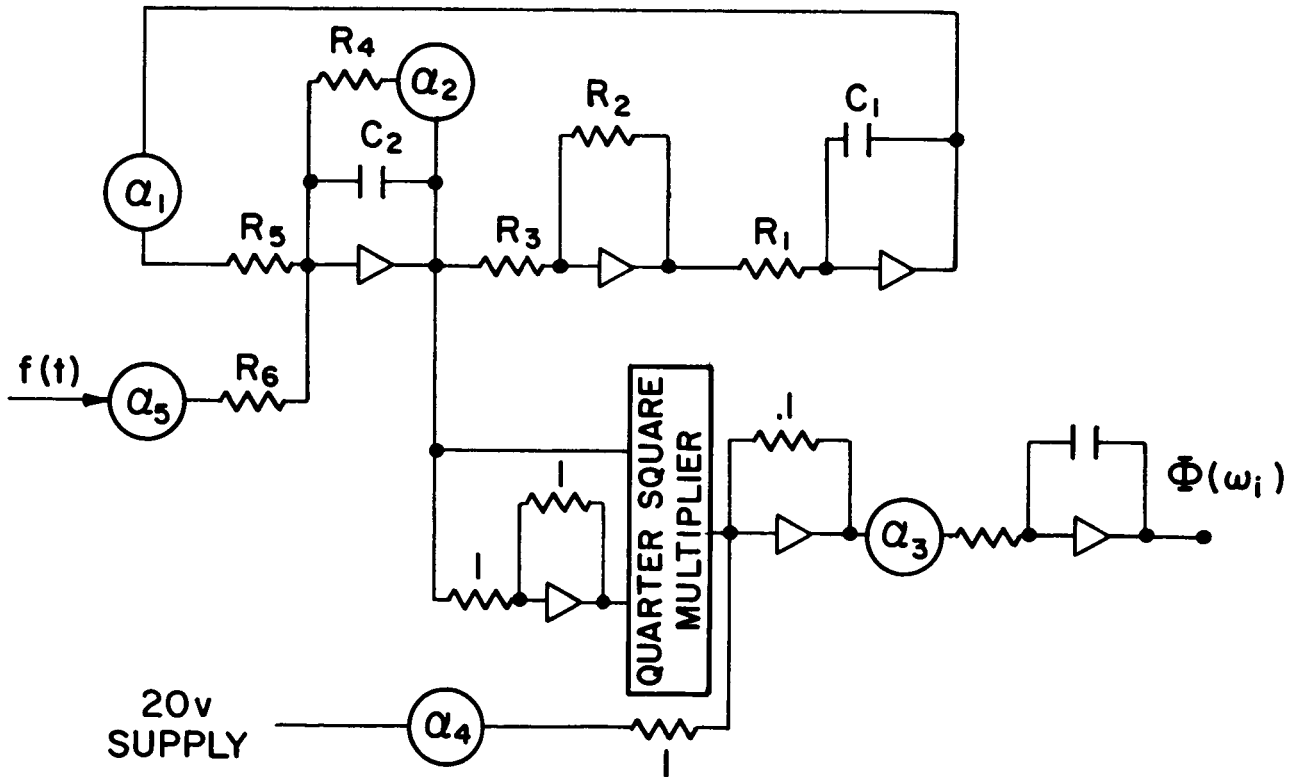acteristics.

Figure 6. Typical Filter, Square, Averaging Analog Circuit

$$\alpha_1 = \frac{2\pi\,\omega_i\,R_4}{R_1\,R_5\,C_1\,C_2} \tag{16}$$

$$\alpha_2 = 4\pi\,\xi\,\omega_i\,C_2\,R_4 \tag{17}$$

Pot 5 scaled the input of each filter such that given an input spectral density with equal power at each ω_i, all quarter-square multipliers would run at full scale.

$$\alpha_5 = 4\pi\,\xi\,\omega_i\,R_6\,C_2$$

Pot 3 compensated for the effects of pot 5 and multiplied the output by the reciprocal of the filter bandwidth (see Equations 2 and 4).

$$\alpha_3 = \frac{1}{B} \tag{19}$$

Pot 4 nulled the zero offset of the multiplier when used as a squaring device.

An additional circuit calculated the total power P_T by averaging the squared input signal.. While this quantity is used as a normalization factor in the spectral analysis, it was also used as a gross measure of the subject's performance.

VI. Error Analysis

Aside from the question of data variability due to a finite averaging time, there exist errors attributable to the accuracy of the spectral analyzer. The computing components of the analog computer are rated at better than 0.1% and system noise level was shown to be at about -37 db (full scale reference) by analyzing a magnetic tape pre-recorded with f(t) equal to zero.

The largest error in the computing system was produced by the quarter-square multipliers. These multipliers were adjusted for a static error of less than 0.15% of full scale. For this type of multiplier the value of the error is a constant and can become significant for small values of the multiplier output. This error could effect the spectral analysis by approximately ±2 db referred to -30 db but has negligible effect near the full scale output. It should be noted that quarter-square multipliers with much higher static accuracy are commercially available.

Several tests were performed to check the accuracy of the circuits. The spectral density function of band-limited white noise as well as a single sinusoid was shown to agree quite closely with the theoretical curves over

a measurement range of about 30 db. The trapizoidal rule area under several of the measured spectral density functions was generally shown to equal 1.0 ±5% indicating accurate operation and proper distribution of the filter center frequencies.

References

Bekey, G. A. Sampled data models of the human operator in a control system. Aeronautical Systems Division Technical Report ASD TDR 62-36, United States Air Force Systems Command, Wright Patterson Air Force Base, Ohio, February, 1962.

Davenport, W. B., Jr., & Root, W. L. An Introduction to the Theory of Random Signals and Noise, New York: McGraw-Hill Book Company, Inc., 1958.

Howe, R. M. Linear systems with random inputs. Unpublished notes, University of Michigan.

Kelly, E. J., Lyons, D. H., & Root, W. L. The sensitivity of radiometric measurements. Journal of the Society of Industrial and Applied Mathematics, 1963, 11, 235-257.

Larrowe, V. L. Bandpass quadrature filters. From Analog Computer Measurement of Time-Varying Power Spectra, Ph. D. Dissertation, University of Michigan, 1964.